JOURNAL OF Applied Polymer SCIENCE

Lignocellulosic Fiber Reinforced Composites: Influence of Compounding Conditions on Defibrization and Mechanical Properties

Johnny Beaugrand,[1,2] Françoise Berzin[1,2]
[1]INRA, UMR614 Fractionnement des AgroRessources et Environnement, F-51100 Reims, France
[2]Université de Reims Champagne-Ardenne, UMR614 Fractionnement des AgroRessources et Environnement, F-51100 Reims, France
Correspondence to: J. Beaugrand (E-mail: johnny.beaugrand@reims.inra.fr)

ABSTRACT: This work describes a systematic study of the compounding conditions by twin-screw extrusion on the defibrization process that modulates the fiber aspect ratio and in turn the mechanical properties. Composites made of polycaprolactone reinforced by 20% hemp fibers were prepared by melt blending. The influence of the extrusion parameters (screw speed, feed rate, barrel temperature, and screw profile) and the initial fiber moisture content on both the fiber dimensions and the mechanical performance of the composite was investigated. The fiber aspect ratio increased when the fibers were water plasticized, principally at a higher feed rate and under a moderated extrusion temperature. The screw speed slightly influenced the fiber dimensions. Flow modeling was used to estimate the specific mechanical energy provided to the fibers, which ranged from 300 to 1700 kWh/t. Independent of the screw profile, a decrease in fiber length with an increase in energy was observed. The evolution of the fiber length and aspect ratios with respect to energy can be accurately described by an exponential function. © 2012 Wiley Periodicals, Inc. J. Appl. Polym. Sci. 000: 000–000, 2012

KEYWORDS: composites; extrusion; fibers; mechanical properties; theory and modeling

Received 30 March 2012; accepted 9 August 2012; published online
DOI: 10.1002/app.38468

INTRODUCTION

Despite their advantageous properties (renewability, low density, satisfactory mechanical properties), lignocellulose (LC) fibers, and natural fiber composites (NFCs) that incorporate LC have not yet been used extensively in the current composite market. Indeed, their natural inhomogeneity and rather unpredictable behavior during transformation processes do not fulfill the industry requirements. We believe that a better understanding of the processing conditions will allow the optimization of the fiber structure geometry and allow the exploitation of these fibers as potential load-bearing bodies. With synthetic glass fibers, a better control of the breaking process may improve the composite mechanical performance, as has been shown previously.[1,2] In this study, bast fibers isolated from the stem of hemp were used because of their widespread in the NFC market. They have the advantage of being strong and stiff, and they are used in interior composites for the automotive sector.[3]

An individual LC fiber can be assimilated into a cell wall organized into a tubular shape with tapered extremities. Those individual unit cell fibers are usually cemented together into bundles (and then into groups of bundles) by a middle lamella that is composed of a matrix made of several amorphous polymers.[4] These amorphous polymers can be hydrophilic (e.g., pectins or hemicelluloses) or more hydrophobic in the case of lignins and their phenol groups. The LC fiber cell wall is a multilayer structure and can therefore be assimilated into a natural composite that is reinforced by cellulose oriented microfibrils with a helical arrangement.[5] This cellulose is embedded in a matrix of amorphous polymers (mostly hemicelluloses and lignins) that are located non-homogeneously.[6] The roles of the amorphous polymers have not been fully elucidated[7]; however, they have been implicated in the stress transfer to cellulose.[8]

The defibrization process concomitantly results in decohesion and fragmentation phenomena of the fiber elements. When fracture occurs in the interfiber cement (i.e., by degumming of the middle lamella connecting fibers), the process is called decohesion. Fragmentation occurs when the intrafiber structure integrity, i.e., the cell wall, is damaged. Defibrization is therefore related to fracture, and initiation sites and propagation pathways can be influenced by intrinsic parameters related to the quality of the fibers as well as by external factors (e.g., machining,[9] stress mode,[10,11] etc.)

At the molecular level, some factors that influence the viscoelastic properties, such as the water (moisture) content and

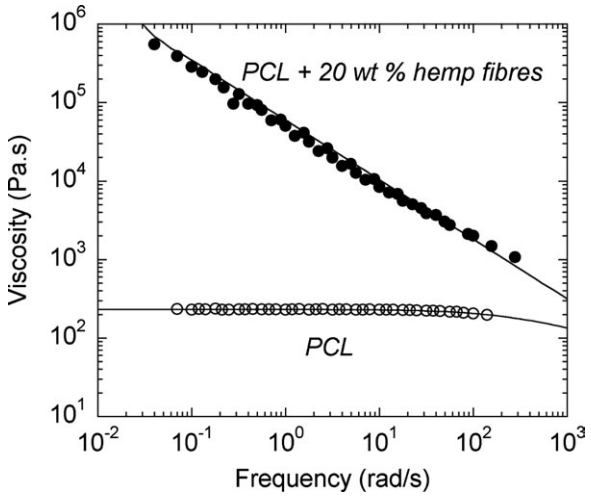

Figure 1. Viscosity curves of PCL and composites (PCL + 20 wt. % hemp long fibers) at 160°C. Symbols are experimental points, full lines are fits by a Carreau–Yasuda law (PCL) or a power law (PCL + 20 wt. % hemp long fibers).

temperature,[7] are known to influence the mechanical behavior of the fiber cell wall. In this study, the fiber amorphous polymers targeted by those factors are lignins[12] and noncellulosic polysaccharides, primarily hemicelluloses.[13] These fiber amorphous polymers can undergo drastic changes from glassy "brittle" to rubbery "ductile" states when the glass-transition temperature T_g is exceeded. Because these amorphous polymers are not uniformly present in the fiber cell wall, local variations in the properties are expected. As a consequence, these variations can potentially modulate the fracture location[14] and, therefore, the defibrization. In the context of this paper, defibrization will occur according to one of three interaction types: between the fibers themselves, between the fibers and extruders (barrel and screws) or between the fibers and the polymer matrix. New insights into LC fiber (flax) rupture have recently been established by their direct observation during compounding with rheo-optics.[15] Rupture by fatigue was evidenced, and the authors confirmed that natural defects initially present strongly influence the rupture location. The aspect ratio Length/Diameter (*L/D*) is a classical way to describe the fiber geometry.[16,17] Keller[18] has demonstrated that individualized hemp bundle fibers that are degummed into single cells exhibit better aspect ratios, *L/D*, when the fibers are more individualized. In addition, the *L/D* ratio can be translated into a potential interfacial area for the prediction of the fiber-matrix adhesion. Furthermore, the aspect ratio of cellulosic fibers compounded by twin-screw extrusion (TSE) has proved to be dependent on the initial fiber concentration.[19] An interesting study reported on the evolution of fiber morphology in an internal batch mixer. With this process, the authors showed empirically the impact of the processing conditions on aspen and wheat-straw fiber geometries, and their results should prove valuable in determining the influence of the TSE processing parameters.[20]

A twin-screw extruder can be seen as a continuous reactor where the mechanical shear, the thermal stress and the residence time can be controlled.[21] In TSE, the total energy provided to the extrudate can be expressed as the Specific Mechanical Energy (SME). We postulate that the SME can be a consistent factor that influences the LC fiber defibrization because the SME input has been shown with glass fiber to determine the fiber breakage during compounding.[22] The SME is difficult to measure accurately. Moreover, the extraction of the portion that is devoted to defibrization from the global SME is experimentally impossible. With the aid of specific software dedicated to TSE,[23] flow simulations can be performed, and the local SME transmitted to compounded components can be estimated. This procedure was used herein for hemp fibers.

Our major objective was to establish a nonempirical control of the defibrization process during compounding by twin-screw extrusion to provide a higher fiber *L/D* ratio. For that, we explored the hypothesis that the viscoelasticity of fiber amorphous polymers can significantly influence the fiber defibrization (fiber decohesion versus fragmentation) and, in fine composites, the mechanical properties. For this reason, TSE experiments were conducted for selected temperature processes with different initial hemp fiber and moisture contents. In addition, a parametric study on the influence of the screw speed, feed rate, barrel temperature, and screw profile on the fiber dimensions was also conducted, and relationships between the processing parameters and the fiber morphology were established.

EXPERIMENTAL

Materials

The matrix selected for this study was a polycaprolactone (PCL), which is a linear bioresorbable and biodegradable polyester.[24,25] PCL has a low melting temperature (60°C), which is desirable in the compounding of LC fibers. Indeed, PCL allows processing at temperatures less than the generally admitted thermal degradation temperature of LC (starting at 160°C). PCL (Capa© 6800) was provided by Perstorp (United Kingdom). It has a molecular weight of 80,000 g/mol and an MFI of 3 g/10 min (160°C, 2.16 kg). At 160°C, its rheological behavior is quasi-Newtonian, and it exhibits a viscosity of 230 Pas (Figure 1). PCL is compatible with a broad range of thermoplastics and is soluble in numerous common solvents. Another interesting property of PCL is its high thermal stability (350°C) and its remarkable processability. Some mechanical properties of solid PCL have been measured and are summarized in section Results and Discussion.

The plant material used in this study came from hemp stems (*Cannabis sativa L.*, variety Fedora 17), which were grown in Aube (France) in 2009 and were supplied by Fibres Recherche Développement® (Troyes, France). To minimize the heterogeneity and length dispersion of the plant material, kilogram quantities of long (decimetric) scutched bast fibers were manually hackled and oriented before being chopped into a homogeneous masterbatch with a length of ~2 cm. Fiber samples tested at different values of moisture content in a twin-screw extruder were preconditioned before testing. They were conditioned at 50, 75, and 90% relative humidity (RH) in a climatic chamber using salt-saturated aqueous solutions for four days at 20°C, which resulted in water contents of 9.8, 14.0, and 22.5%, respectively. During conditioning, aliquots of 100 g (dry matter basis) of the fibers were placed into open double plastic bags before being

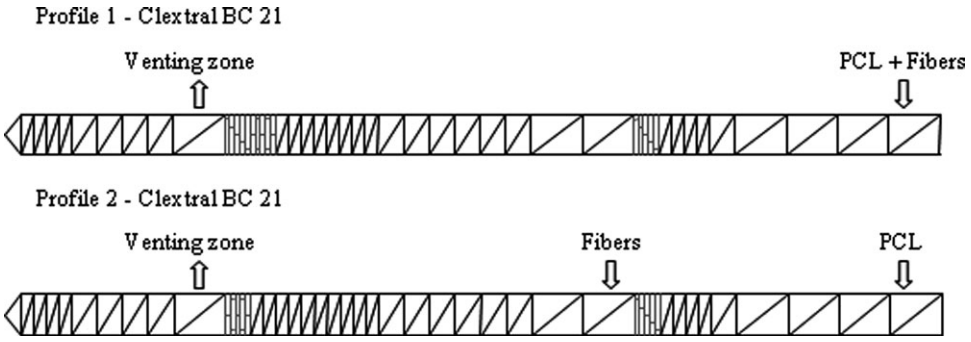

Figure 2. Screw profiles used (blocks of kneading discs in gray).

sealed and later fed into the twin-screw extruder. The moisture content of the hemp fibers before extrusion or the moisture content of those extracted from PCL after extrusion were determined through assessment of the moisture loss by the drying material at 80°C for 48 h in an oven. All data are expressed on a dry matter basis.

Thermogravimetric analyze (TGA) characterization of the native hemp fibers were done by following the variation of mass vs. temperature. TGA was performed at 5°C min^{-1} on a SDT Q600 apparatus from TA Instruments (USA). The analyze was carried out under N2 atmosphere on a sample of ~20 mg from 20 to 550°C.

Extrusion Conditions

Composites were prepared using a Clextral BC 21 (Firminy, France) laboratory-scale twin-screw extruder with a diameter D of 25 mm and a length L of 900 mm (L/D ratio: 36). Two different screw profiles were used (Figure 2), both of which included a venting zone for the evacuation of water steam. Profile 1 had two blocks of kneading discs: the first block had staggering angles of −45°, and the second one had angles of 90°, followed by −45°. In this case, PCL and hemp fibers were introduced simultaneously into the hopper. Profile 2 also had two blocks of kneading discs, but the second was less severe in this case (its length was divided by two, and it was staggered at 90°). Moreover, in this case, the hemp fibers were introduced into the second hopper (in barrel 4) after the PCL had melted. Consequently, the extrusion conditions with Profile 2 were much less severe than those with Profile 1. Profile 1 was used to study the influence of the fiber moisture content (9.8, 14.0, and 22.5%) and the barrel temperature (100 and 140°C) under fixed processing conditions (screw speed N = 250 rpm, feed rate Q = 0.85 kg/h). Profile 2 was used at a fixed RH value of 50% and at a fixed barrel temperature of 100°C to quantify the processing effect of using different screw speeds (100–400 rpm) and feed rates (0.85 and 1.5 kg/h). All the extrusion conditions tested are listed in the Table I.

The fibers were mixed with a PCL matrix at a concentration of 20 wt %. Preliminary experiments carried out in our laboratory shown that higher fiber concentration (i.e., 30 wt %) was not realistic to preserve an accurate feeding with the volumetric feeder (KCV-KT20, K-Tron, Niederlenz, Switzerland) we used. Indeed, a constant dosing of long centimetric fibers is nearly impossible upper 20 wt % because the fibers build up entanglements with a strong cohesion. At 40 wt %, these long fibers can even block the screws of the feeder. We therefore have adopted a low feed rate of 20 wt % in all experiments. Moreover, to be certain to prevent the possibility of irregular fiber feeding that usually occurs with long fibers or low-density materials,[26] a homogenous feeding manual adjustment (i.e., removing by hand the large fiber bundles in the hopper) was performed on the feeder when necessary.

Flow Modeling

To estimate the values of the parameters that cannot be measured during the compounding process, we used the Ludovic© flow simulation software, which is dedicated to twin-screw extrusion.[23] In the present study, Ludovic© was principally used to estimate the specific mechanical energy (SME) transmitted to the composite during compounding with hemp fibers.

Composite Characterization

After extrusion, the composite strands were cooled down at room temperature. For each set of conditions examined, a sample of 10 composite pieces ~10 cm apart from each other and weighing ~2 g were collected from the extrudate. The PCL matrix was then Soxhlet extracted, as described below, to

Table I. Process Parameters for Extrusion (Clextral BC 21)

	Moisture content (%)	Screw speed (rpm)	Feed rate (kg/h)	Barrel temperature (°C)
Profile 1	9.8	250	0.85	100
	14	250	0.85	100
	22.5	250	0.85	100
	9.8	250	0.85	140
	14	250	0.85	140
	22.5	250	0.85	140
Profile 2	9.8	100	0.85	100
	9.8	200	0.85	100
	9.8	300	0.85	100
	9.8	400	0.85	100
	9.8	100	1.5	100
	9.8	200	1.5	100
	9.8	300	1.5	100
	9.8	400	1.5	100

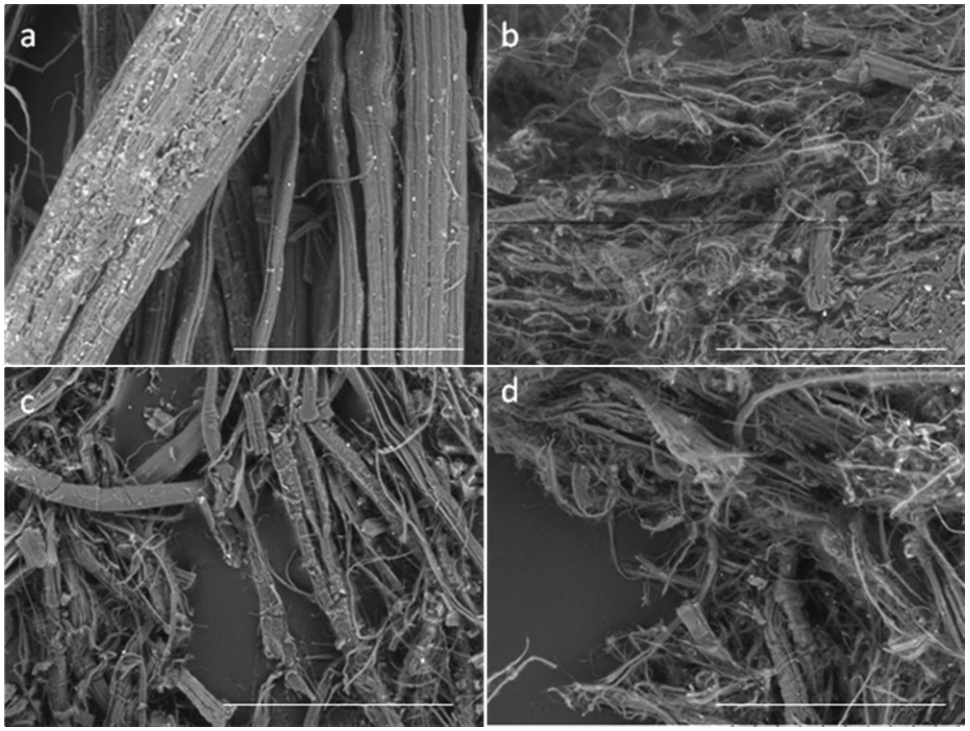

Figure 3. Micrographs of representative's fiber populations visualized by Scanning Electron Microscope (SEM). (a) is the initial hemp fiber fraction, very large bundles are visible and the fraction is characterized by a *L/D* ratio of 310. (b), (c) and (d) are extruded fibers, further extracted from the PCL matrix. (b) and (d) are two illustrations of the extremes average fibers *L/D* values with 17 and 39 respectively. In (b), bundles are no longer visible when rare intact fiber units are still visible, the overall is highly destructured, whereas in d the defibrization process results in a fiber unit predominance. (c) is a intermediary *L/D* value of 24, and a more balanced ratio of bundles and fiber units is seen. Scale bars = 200 μm in (a), (b), (c) and (d).

determine the fiber content. These values allowed the evaluation of any fiber content variations during the compounding process and allowed verification that the average value satisfied a 20% target. Soxhlet extractions were performed over two days while refluxing at ~45°C in dichloromethane.

The composite strands were ground, and standard dumbbell specimens (ISO 527–2–5 A) were injected using an injection molding machine (DK Codim NGH 50/100) at 80°C for the PCL or PCL/fiber composites. The injection-molded specimens were 75 mm long and 2 mm thick and were stored under constant conditions (50% RH, 20°C). The tensile properties in uniaxial extension were measured on a TEST 108 2 kN universal testing machine (GT-TEST, France) equipped with a 500 N load cell piloted by the Testwinner 220 software program. A minimum of 10 samples for each composite was used, and the average value was reported. The tensile failure stresses were measured at a crosshead speed of 10 mm/min under constant storage conditions (50% RH, 20°C) in an environmentally controlled instrument room.

Fiber Element Dimensions

The micrographs of representative's fiber populations were visualized by Scanning Electron Microscope (SEM) with a tabletop microscope (TM-1000, Hitachi, Tokyo, Japan). No coatings of the samples were required for observing the samples at the magnification presented (×400).

The extracted fiber dimensions and morphologies were obtained by image analysis via optical microscopy capture and the MorFi© software package (Techpap, Grenoble, France). This well-established methodology is currently used in pulp and paper applications and provides morphological characteristics that are suitable for the present study. Diluted fiber suspensions of 1 g were tested in duplicate or triplicate, and the mean values are provided. More than 100,000 elements were counted for each composition, which provided a statistically significant panel of populations. By convention, MorFi© has set thresholds under which elements with lengths greater than 200 μm are considered fibers and smaller elements are otherwise considered fine particles. The fiber elements are further characterized by their aspect ratio, *L/D*, where *L* is the length, and *D* is the diameter.

Various types of methods are available for studying the fiber dimensions, and their advantages and drawbacks must be discerned. The method, which may range from "by hand" to "fully automated," is well known to influence the measurement and shape distribution of fibers, as has recently been investigated in depth.[27] Here, we have preferred the statistical significance (more than 100,000 elements analyzed) of the "commercial automated" versus the "laboratory made" systems. We have thus chosen the MorFi© system. We are aware that, from one system to another, "absolute" length values do not exist, and 20% variance is typical.[28] In this study, the hemp fiber length and diameter distributions measured by the MorFi© optical fiber dimension analyzer system showed Gaussian-type distribution trends,

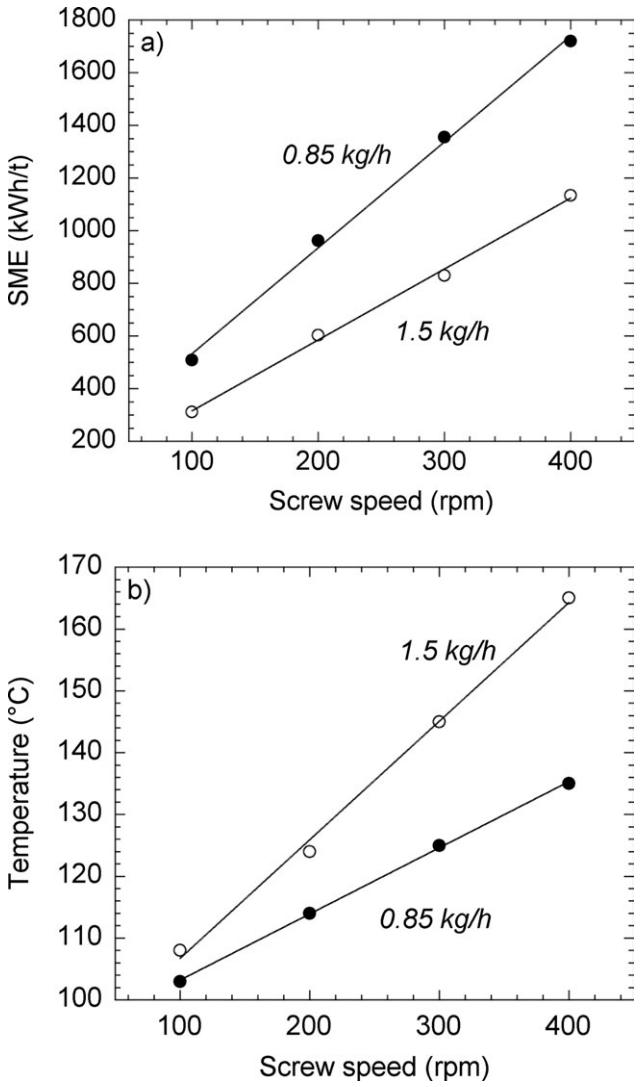

Figure 4. Change in the SME (a) and the final temperature (b) with the screw speed for two different feed rates.

irrespective of the TSE conditions tested (data not shown). Therefore, for the sake of clarity, we commonly use the average fiber length or diameter in the following sections. Interestingly, Le Moigne et al.[27] concluded from a study on three types of fibers that the length distribution did not exactly follow a lognormal law. To explain this difference with our results, we hypothesize that the hemp fibers we used can differ from the flax, sisal and wheat straw sources they used. In addition, they also reported a marked influence of the fiber typology on the evolution profiles during compounding, and a divergent behavior for hemp cannot be excluded. Compared to the length of the starting fiber elements (20 mm), the extruded fiber lengths were drastically reduced, by an average of 40-fold, for the different trials (Figure 3). In addition, we observed a width reduction for the fiber elements, with values ranging from 75 to 10 μm (data not shown).

RESULTS AND DISCUSSION

The morphology of conventional glass fiber composites[1] and that of WPC[29] have been shown to be affected by TSE compounding. Although interest in adjustment of the fiber length and aspect ratio have been addressed for the optimization of the reinforcement with glass fiber composites and WPC, which are homogeneous materials,[2] the question remains open for natural fibers.[17] because they are heterogeneous by nature. The LC fiber defibrization behavior is known to be influenced by intrinsic properties as well as by external conditions. A previous study focused on the influence of various LC microstructures on the properties of composites processed by extrusion.[14] Here, we have modified the previous approach by using one LC fiber microstructure and studying the fiber aspect ratio, *L/D*, in composites. This modification followed two approaches: in the first approach, the fiber water content and the temperature of the process, both of which influence the mobility of the fiber/amorphous polymers, were modulated; in the second approach, the influence of the TSE processing parameters were explored. We then proposed original relationships between the fiber length or the *L/D* ratio and the composite mechanical performances.

Extrusion Conditions

As a first step, we considered the TSE conditions to define the thermomechanical treatment applied to the hemp fibers during the compounding process. We focused on two major processing conditions known to impact synthetic fiber morphology,[22] including the effects of the screw speed, *N*, and feed rate, *Q*, on the hemp fiber for Profile 2. The combined effects of the screw speed and the feed rate are often represented as a function of the SME. Indeed, the SME can be easily measured on a twin-screw extruder and is usually proportional to the ratio of the screw speed to the feed rate (*N*/*Q*). Figure 4(a) shows that the SME increases linearly with the screw speed and is more important at low feed rates. The high values obtained here (300–1700 kWh/t) are principally due to the low values of the feed rates. Indeed, because of difficulties with the correct feeding of the centimetric hemp fibers, only low feed rates were attainable. Consequently, the composite temperature at the die exit is also largely dependent on the processing conditions, as shown in Figure 4(b). It increases linearly with the screw speed and is higher for the highest feed rate. If we compare the evolutions of the SME and temperature for the same SME, the temperature is highest with the highest feed rate. This result can be explained by a shorter residence time under these conditions, which results in a reduced heat transfer toward the barrel at 100°C.

To access other parameters of the extrusion process, we used the Ludovic© modeling software.[23] For this purpose, the viscosities of the PCL and the composite with 20 wt. % fiber needed to be determined. These values were measured on a parallel-plate rheometer with small-amplitude oscillatory shear, and the results are shown in Figure 1. The PCL is Newtonian over a wide frequency range (0.1 to 50 rad/s) and exhibits a moderate shear-thinning behavior at frequencies greater than 50 rad/s. The behavior of the PCL can be correctly described by the Carreau-Yasuda law, with a zero shear viscosity of 230 Pa.s, a power law index of 0.65 and a Yasuda parameter of 0.94. Similar behavior was observed by Gimenez et al.,[30] who obtained values of 0.52 for the power law index and 1.05 for the Yasuda

Applied Polymer SCIENCE

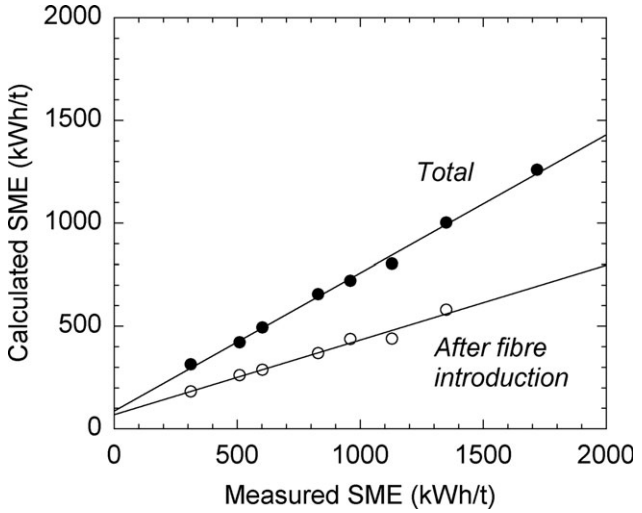

Figure 5. Comparison between the calculated and the measured total SME and between the total and local (after fiber introduction) values.

parameter. In contrast, the composite exhibited a power law behavior with a significantly higher viscosity (approximately 52,000 Pa.s at 1 rad/s) and a power law index of 0.25. Similar power laws have been frequently observed for highly filled systems.[31] Flow simulations were made for the various trial conditions. Using the Ludovic© software, we calculated the total SME of the whole process, which can be compared to the experimentally determined SME that was deduced from the motor torque. We also calculated the local SME that is added to the composite after the introduction of the fibers and which cannot be measured. In Figure 5, we compare the calculated SME with the experimental values for all the experiments performed with profile 2 (i.e., varying the screw speed and feed rate). The model correlates to the measured values, even though it tends to underestimate them. The results also show that the local energy provided to the fibers is proportional to the global value, but is only 56% of the global SME. Because the data in Figure 5 have been obtained for various screw speeds and feed rates, we assume that this ratio is valid, irrespective of the processing conditions. Consequently, we used this value to quantify the SME received by the fibers starting from the measured SME values.

Fiber Element Dimensions

Influence of Fiber Humidity and Barrel Temperature. Before compounding, the fibers were preconditioned at different RH values of 50, 75 and 90%, which correspond to water contents of 9.8, 14.0 and 22.5% ± 0.4 (dry matter based), respectively. The fiber water content is an important factor because water acts as a plasticizing agent[12] and can thus affect the fiber polymer mobility and, consequently, the breakage conditions.[13] For example, hemicellulose-based films exhibit brittleness at low moisture contents. Our experimental data show that the fiber length increases proportionally with the moisture content and is superior at lower temperatures [Figure 6(a)]. Similar results were obtained with the *L*/*D* ratio [Figure 6(b)], which ranged from 14 to 26; these results demonstrate that the fiber humidity and the temperature during extrusion both influence the fiber defibrization. These results are original and support our initial hypothesis that the mobility of fiber amorphous polymers can be modulated for acting on defibrization mechanisms. Notably, these amorphous polymers are preferentially located in the interfiber cement that gives cohesion to the bundles. These amorphous polymers can be more mobile according to the extrusion temperature and their glass-transition temperature T_g, and consequently they can be more or less brittle. As illustration, the amorphous polymer mobility modulation can drastically changes the mechanical properties of many polymers as reported for the Young's modulus at approximately the polymer's T_g.[32] Furthermore, their mobility is increased by plasticizing effects with increasing water content.[12,33,34] The mechanical properties are thus affected. For instance, a 10-fold decrease in the ultimate stress of a biopolymer was measured when tested at 60 versus 90% relative humidity.[35] The mobility increase could, in turn, favor fiber separation by an interfiber longitudinal decohesion and limited intrafiber damage, i.e., fragmentation with the fracture direction along the cell wall. This separation would theoretically give a higher *L*/*D* ratio, as supported by our experimental results

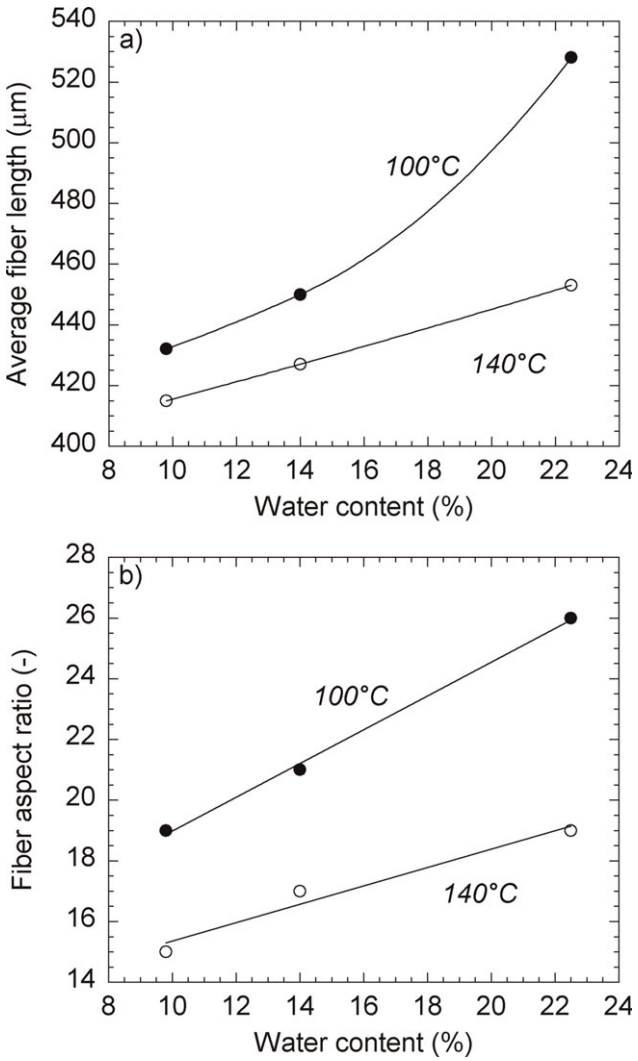

Figure 6. Change in the fiber length (a) and the fiber aspect ratio, *L*/*D* (b) with fiber moisture content at two barrel temperatures (Profile 1, 0.85 kg/h, 250 rpm).

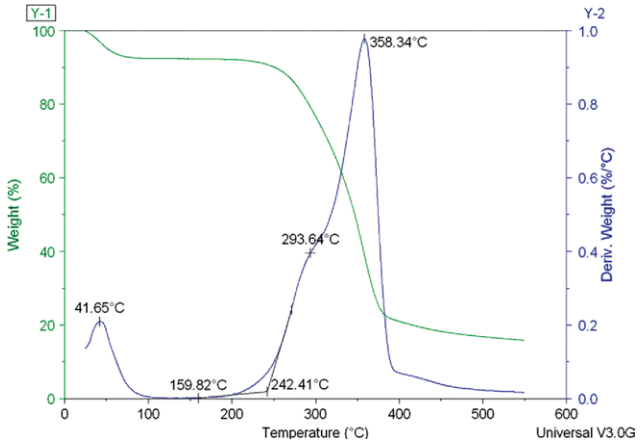

Figure 7. Thermogravimetric analyze (TGA) characterization of the native hemp fibers. Variation of mass vs. temperature measured by TGA conducted at 5°C min-1 shows the beginning of degradation of the native fibers at about 160°C. [Color figure can be viewed in the online issue, which is available at wileyonlinelibrary.com.]

(Figure 6). At a low moisture content, based on changes in the polymer mechanical properties, less softening of the fiber unit or bundles is expected.[36] In addition, at a low water content, defects induced by the process or already naturally present in the cell walls of the fiber structures can initiate more intrafiber fractures, i.e., fragmentation, as has been reported for wood.[37]

For the same reasons as previously detailed regarding the influence of water, the fiber length and *L*/*D* ratio are expected to increase with a higher barrel temperature [140°C compared to 100°C, Figure 6(b)]. However, the opposite trend was observed. This result can be explained by a partial thermal degradation of the fiber polymers. Indeed, with a fiber residence time of approximately 220 s, a degradation of the polymers cannot be excluded, which would explain this unexpected behavior. In addition, the calculated local temperature within the twin-screw extruder can be greater than 160°C, lignins and non-cellulosic polymers are generally considered to degrade in this range. To verify this assumption, we tested raw fibers stability using Thermo Gravimetric Analysis. We observed a beginning of mass loss not related to water behind a temperature of 160°C (Figure 7). This onset of mass loss indicates that some fibers components were altered from this temperature. Because the amorphous polymers are the more thermo-labile components in our context, this strongly suggests that our hypothesis about a beginning of amorphous polymer degradation is correct, and especially if one remember that the fibers residence time in the extruder is quite long (~220 s).

Influence of Processing Conditions. Processing conditions are known to influence fiber morphologies. This influence has been reported for carbon fibers,[38] glass fibers,[1,22] and also LC fibers.[18,29] For example, a better longitudinal separation was observed with flax fibers compared with other LC resources[14] when extruded. Figure 8(a) shows the effect of various screw speeds and feed rates on the fiber length for composites prepared under Profile 2 (100°C, 9.8% moisture content). Although we did not observe a clear effect of these parameters on the fiber length, a tendency can be deduced. An increase in the screw speed tends to decrease the fiber length. This effect can be observed independently of the feeding rate, irrespective of the matrix and the nature of the fiber, as was partially confirmed by a recently reported work performed with a TSE[39]that contradicts data produced from an internal batch mixer.[40] Identifying the causes responsible for this discrepancy is unfortunately not possible here. It would have been possible by an in-depth comparison of the different experiments, if the *L*/*D* ratio had been given according to a common measurement unit, like the SME.

The fiber length values are higher with feed rates of 1.5 kg/h compared to 0.85 kg/h. Our results are in agreement with what is typically observed for glass fibers, whose length is reduced during compounding when the screw speed is increased and the feed rate is decreased.[22] The influence of the screw speed can be explained by an increase in the shear stress, where the influence of the feed rate is related to the decrease in the residence time. Surprisingly, the fiber length and the fiber aspect ratio, *L*/*D*, are

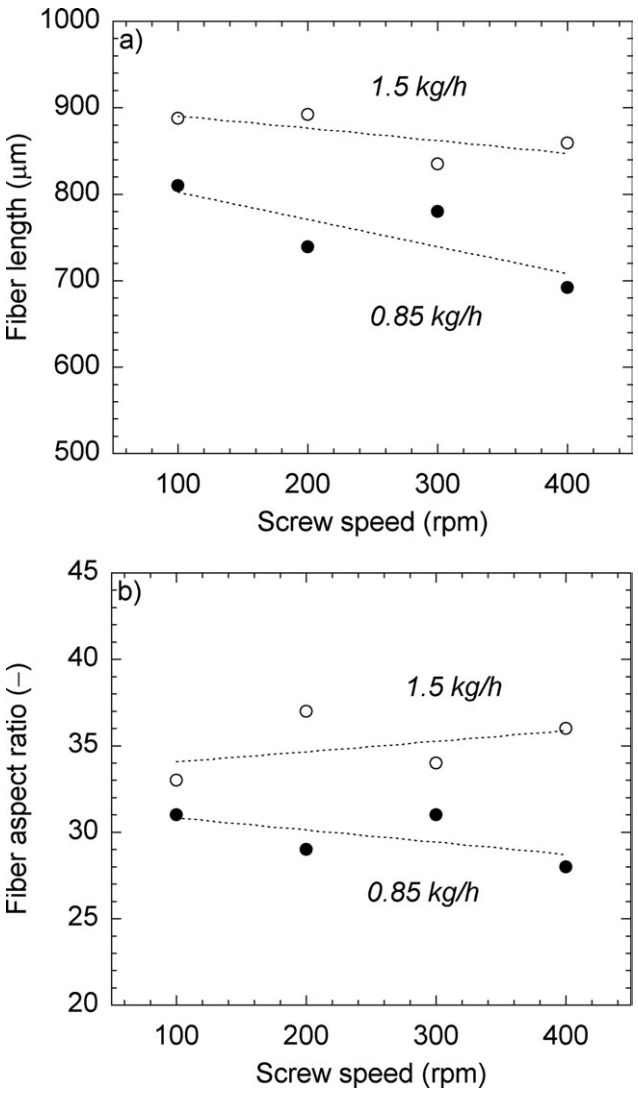

Figure 8. Change in the fiber length (a) and the fiber aspect ratio, *L*/*D* (b) with screw speed at two feed rates (Profile 2).

Applied Polymer SCIENCE

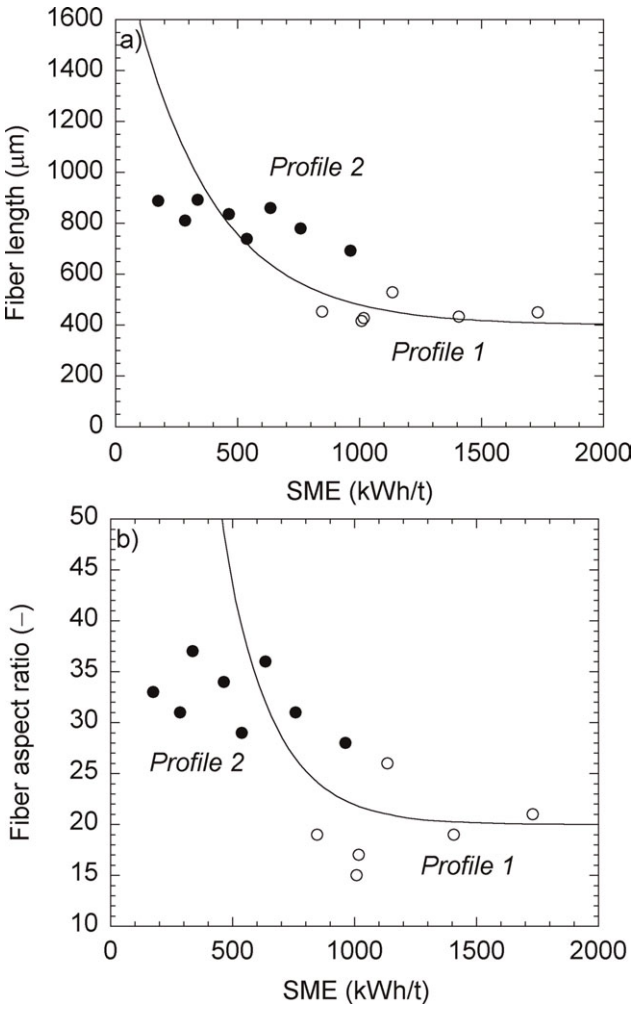

Figure 9. Change in the fiber length (a) and the aspect ratio, *L/D* (b) with specific mechanical energy (SME) for the two screw profiles. Symbols are experimental points. Full lines are the fit by the model.

affected differently by the screw speed. Indeed, an increase in the screw speed results in a moderate decrease in the fiber length, which is more pronounced for a rate of 1.5 kg/h, whereas the aspect ratio, *L/D*, appears unchanged. This result suggests that the fiber element diameters are reduced at an unrelated rate relative to the fiber lengths. In other words, decohesion that results in the longitudinal separation of hemp fibers (*L/D* ratio increases) occurs according to a mechanism that differs from that of fragmentation (intrafiber, *L/D* ratio decreases) with respect to the screw speed and the feed rate [Figure 8(b)].

Glass fiber breakage during compounding has recently been shown to be related to the SME.[22] Figure 9 represents the effects of the SME on the fiber length and the *L/D* ratio. For Profile 2, we have considered the local SME, dissipated after the introduction of the fiber elements. Independent of the screw profile, we observe a decrease in fiber length followed by a plateau above 1500 kWh/t. This profile is similar to that observed for glass fibers. As proposed by Inceoglu et al.,[22] we can fit these results to an exponential function of the form:

$$L = L_\infty + (L_0 - L_\infty)\ \exp(-K.\mathrm{SME})$$

where L is the fiber length, L_0 is the initial value, $L_{\infty\ is}$ the limit value, and K is a constant. As evident in Figure 9(a), this function allows a correct description of the fiber evolution (regression coefficient = 0.92), with $L_0 = 2000$ μm, $L_\infty = 400$ μm and $K = 0.003$ (kWh/t)$^{-1}$. A K value of 0.2 (kWh/t)$^{-1}$ was obtained by Inceoglu et al.[22] for glass fibers, which indicates that brittle fibers can be more easily broken during extrusion. A similar, though more scattered, exponential evolution (regression coefficient = 0.91) may also be obtained for *L/D* [Figure 9(b)] with following values: $L/D_0 = 310$, $L/D_\infty = 20$, and $K = 0.005$ (kWh/t)$^{-1}$.

Mechanical Properties of Composites

General Results. To ensure that all of the composites produced were reinforced with identical hemp fiber contents, we characterized the average fiber content as well as the fiber dispersion along the extrudate. Only experiments with variations less than 10% were considered. Unfilled PCL was first characterized. We obtained a Young's modulus of 90.5 MPa and a stress at break of 15.5 MPa, in accordance with the literature.[41] For composites, the values originated from tensile tests made on standard dumbbell specimens (ISO 527–2–5 A) after injection molding, whereas the fiber dimension analyses originated from the composite extrudates before injection. We therefore admit that the fiber dimensions are generally overestimated when the mechanical performances measured after injection are considered, as this process could also lead to defibrization. However, because no satisfying alternative for material testing was available, we chose to focus on the fiber dimensions immediately after extrusion, instead of analyzing fibers extracted from the dumbbell specimens after an injection step. This strategy has been previously followed for curaua fibers,[39] and, *a posteriori*, the relationships obtained between the fiber dimensions and mechanical properties suggest that this was a sound technical choice. All composites filled with 20% hemp fiber were stiffer and less ductile than those without hemp fiber, as has been generally observed for fiber-reinforced composites. All these data on Young's modulus and stress at break were obtained with a standard deviation around 1 % or less. In this study, no extra information was obtained from the strain at break measurements; we therefore did not present them and instead focused on the Young's modulus and the stress at break values, which increased by approximately 2 to 3 times compared to those of pure PCL (Figure 10). These composites achieved properties seem encouraging for some possible applications; the achieved weight savings and the use of an renewable resource open to a wide range of markets, in particular for automotive interiors like trunk liners or interior door covers.

Influence of Fiber Humidity and Barrel Temperature. The fiber initial moisture content was expected to lead to composite voids and thus to a bias in the measured mechanical performance. To prevent this bias, a venting zone was opened on the TSE at a convenient location (Figure 2) to eliminate the steam generated. The moisture content represented only 2–4.2 g per 100 g of composite for conditions with fibers equilibrated at 9.8 and 22.5% water contents, respectively. The efficiency of the

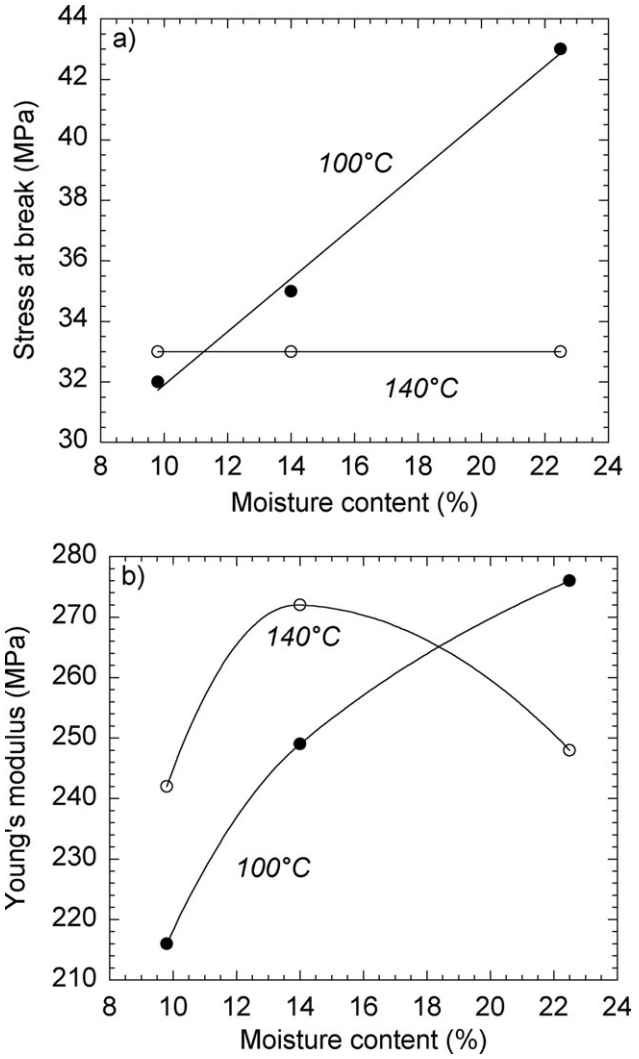

Figure 10. Change in the stress at break (a) and the Young's modulus (b) with the fiber moisture content at two barrel temperatures (Profile 1, 0.85 kg/h, 250 rpm).

venting zone was proved according to two results. First, when the fibers were extruded at 100°C, higher fiber moisture contents resulted in higher mechanical properties (Figure 10). The presence of voids would have generated the opposite results.[42] Second, for each of the three initial moisture contents, we ran a comparative micro-tomography investigation in composite standard dumbbell specimens (Skyscan 1076, France, 6 mm^3 checked at a resolution of 18 μm). As expected, few voids were observed (data not shown), and, more importantly, no void volume variation was seen among the samples. This last result led us to exclude a void bias in our mechanical results. Composites processed at 100°C showed a proportional increase in the stress at break values relative to the moisture content [Figure 10(a)]. An increase in the barrel temperature to 140°C did not result in an observed increase in the stress at break values in the examined range of moisture contents. The change in Young's modulus with the moisture content appeared non monotonous [Figure 10(b)] and the interpretation remains open. At 100°C, the results are consistent with the change in fiber length shown in Figure 6: an increase in the moisture content apparently preserved the length of the fiber elements or favored decohesion, which led to improved mechanical properties. At 140°C, the water influence was less evident. One explanation for this difference is that a thermal degradation of the fiber amorphous polymers occurred (discussed in subsection Influence of processing conditions) due to local temperature elevations. In this case, the fiber reinforcement potential would be reduced, and this reduction coincides with our observations.

According to the fiber aspect ratio, *L*/*D*, the stress at break increased [in Figure 11(a)] only when the composites were processed at 100°C. The *L*/*D* ratios obtained for composites processed at 140°C were generally smaller than those of composites processed at 100°C, and the stress at break values increased with increasing *L*/*D* ratios from a threshold value of 20, which was precisely the highest *L*/*D* ratio obtained at 140°C. At similar *L*/*D* ratios of 20, similar stresses at break were obtained for the two composites, even though they differed in their processing temperatures (100 versus 140°C) and initial fiber moisture

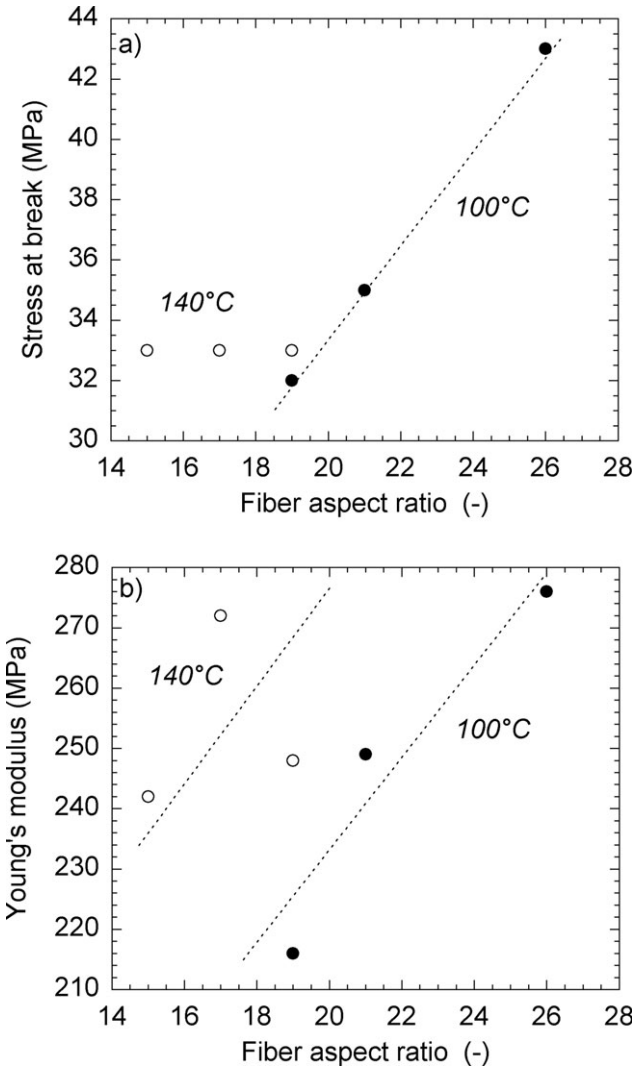

Figure 11. Change in the stress at break (a) and the Young's modulus (b) with the fiber aspect ratio (Profile 1, 0.85 kg/h, 250 rpm).

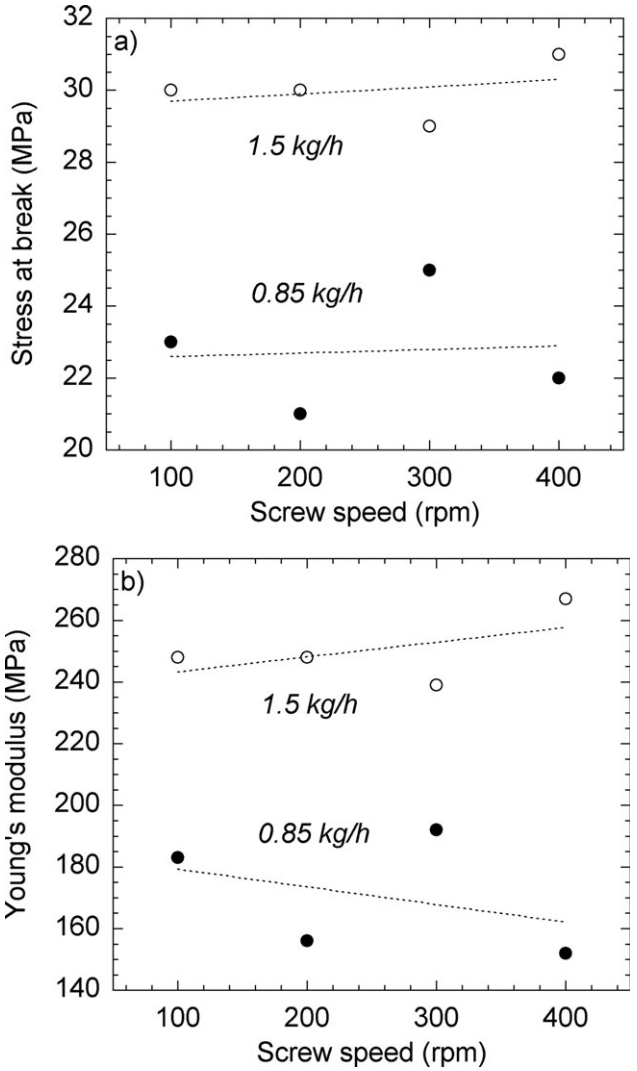

Figure 12. Change in the stress at break (a) and the Young's modulus (b) with the screw speed at two feed rates (Profile 2).

contents (9.8 versus 22.5%) [see Figure 6(b)]. By homology with flax, where a critical aspect *L/D* ratio of 27 was found,[43] we propose that the *L/D* ratio of 20 found herein corresponds to this criteria in hemp. For *L/D* ratios above 20, the composite reinforcement is increased. The Young's modulus did not follow a pattern [Figure 11(b)], which is similar to that of the stress at break. If a trend seems visible for the fibers processed at 100°C, no relationship between the stiffness and the *L/D* ratio appeared with processing at 140°C. This result is in agreement with the Young's modulus/fiber moisture content observations [Figure 10(b)].

Influence of Processing Conditions. The evolution of the mechanical properties with the screw speed for the two tested feed rates showed a slight influence of the screw speed (Figure 12). The feed rate seems to play a more important role because composites were stiffer at higher feed rates. These changes in mechanical properties were qualitatively similar to the changes in the fiber aspect ratio presented in Figure 8. When the mechanical parameters were plotted as a function of the fiber *L/D* ratio (Figure 13), the stress at break and the Young's modulus values were observed to increase with increasing *L/D* ratios. Moreover, if the results obtained with the two screw profiles (Figure 14) are compared, the same properties were not obtained for the same given aspect ratio. The Young's modulus and the stress at break values are higher in Profile 1, which corresponds to the more severe of the two tested profiles. The SME applied to the fibers in Profile 1 covered 800 to 1800 kW/t, whereas a range of 200 to 900 kW/t was obtained with Profile 2 (see Figure 9). The fiber lengths obtained by the two profiles generally differ by a factor two: lengths of 400 µm were observed for Profile 1 and 800 µm for Profile 2. Profile 1 also showed lower *L/D* ratios and was expected to generate lower composite mechanical properties relative to those of Profile 2 with the higher *L/D* ratios. Surprisingly, the experimental data did not confirm this prediction, especially for the stress at break [Figure 14(a)]. The lower *L/D* ratio from Profile 1 resulted in higher resistance. One explanation is that, even though we showed that the fiber *L/D* ratio is a key parameter (Figure 13),

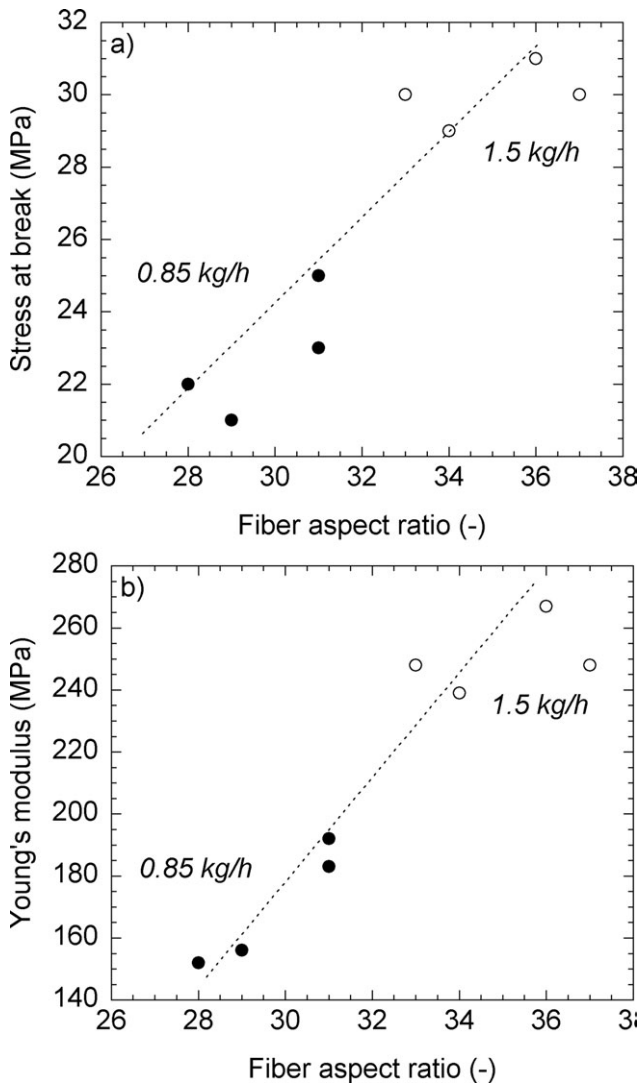

Figure 13. Change in the stress at break (a) and the Young's modulus (b) with the fiber aspect ratio (Profile 2).

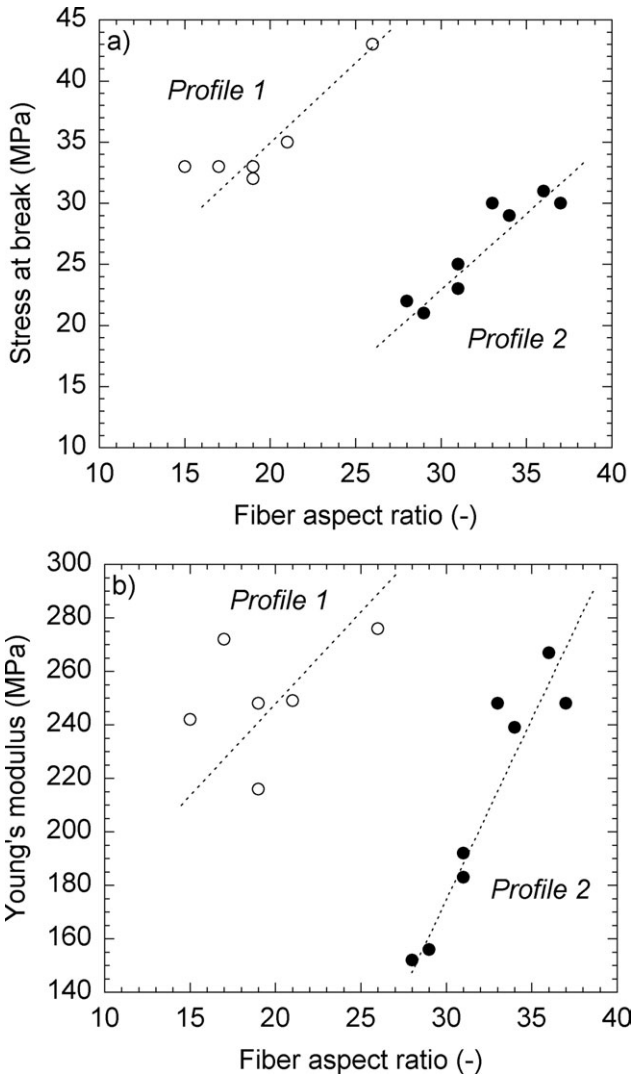

Figure 14. Change in the stress at break (a) and the Young's modulus (b) with the fiber aspect ratio for the two screw profiles.

the *L/D* ratio does not give a full description of the fiber/bundle dimensions. Indeed, at similar *L/D* ratios, the length and the diameter of the fiber/bundle can vary and thus so can its volume. We suggest that the fact that Profile 1 led to greater defibrization of the initial bundles should result in smaller-sized fibers/bundles, and a greater number of interfaces would be created for stress transfer. The composite properties increased as a result. In addition, we also know that the *L/D* ratio imperfectly describes certain structural defects, such as the microcompression/kinks and flaws and the external fibrillations that can weaken the structure.[44] These parameters have not been addressed in this study. Further experimental work is still necessary to adapt the LC fibers into current processes that were initially dedicated to synthetic fibers to increase the composite end-use performance.

CONCLUSIONS

We have prepared composites made of PCL and hemp fibers that were plasticized differently with water according to a twin-screw extrusion parametric study. A significant improvement of the tensile properties of the matrix was obtained with the 20 wt % hemp fiber fraction. Both the Young's modulus or stress at break were doubled or tripled when compared to the neat PCL, depending on the extrusions conditions. We characterized both the fiber dimensions and the mechanical composite properties. We provided evidence that the fibers are subject to severe defibrization (decohesion and fragmentation) during the extrusion process and that a composite mechanical enhancement is achievable through consideration of the fiber factor ratio (*L/D*). In this respect, we have reported originals results demonstrating that greater water plasticization of the fiber results in a higher fiber *L/D* ratio by favoring interfiber decohesion. We varied the extrusion process, which was characterized by the specific mechanical energy. At similar SMEs, the defibrization can drastically differ according to the screw profile. This difference in defibrization affects the fiber *L/D* ratio, which, in turn, influences the mechanical properties of the final composite. Finally, the major novelty brought by this study is the relationships proposed between the fiber aspect ratio, the SME and mechanical properties.

ACKNOWLEDGMENTS

The authors are thankful for the financial support from the MATOREN state-to-country program, France. Patrice Dole (INRA) and Bruno Vergnes (MINES ParisTech) are gratefully acknowledged for their helpful advice and Pr. Vincent Barbin (URCA) for SEM facilities. The authors thank FRD (Troyes, France) for providing the hemp fibers, and Alain Lemaitre, Chang-Pi-Hin Florent, and Nathalie Dehaye for their assistance.

REFERENCES

1. Shon, K. J.; White, J. L. *Polym. Eng. Sci.* **1999,** *39*, 1757.
2. Yoshihara, N. *J. Polym. Eng.* **2006,** *26*, 547.
3. Holbery, J.; Houston, D. *JOM* **2006,** *58*, 80.
4. Andersons, J.; Porike, E.; Sparnins, E. *Compos. Pt. A-Appl. Sci. Manuf,* **2011,** *42*, 543.
5. Barber, N. F.; Meylan, B. A. *Holzforschung* **1964,** *18*, 146.
6. Akerholm, M.; Salmen, L. *Holzforschung* **2003,** *57*, 459.
7. Salmen, L.; Burgert, I. *Holzforschung* **2009,** *63*, 121.
8. Cosgrove, D. *J. Plant Cell* **1997,** *9*, 1031.
9. Medina, L., Schledjewski, R.; Schlarb, A. K. *Compos. Sci. Technol.* **2009,** *69*, 1404.
10. Stanzl-Tschegg, S. E.; Navi, P. *Holzforschung* **2009,** *63*, 139.
11. Marchal, R.; Mothe, F.; Denaud, L. E.; Thibaut, B.; Bleron, L. *Holzforschung* **2009,** *63*, 157.
12. Bouajila, J.; Dole, P.; Joly, C.; Limare, A. *J. Appl. Polym. Sci.* **2006,** *102*, 1445.
13. Bag, R.; Beaugrand, J.; Dole, P.; Kurek, B. *Holzforschung* **2011,** *65*, 239.
14. Oksman, K.; Mathew, A. P.; Långström, R.; Nyström, B.; Joseph, K. *Compos. Sci. Technol.* **2009,** 69, 1847.
15. Le Duc, A.; Vergnes, B.; Budtova, T. *Compos. Pt. A-Appl. Sci. Manuf.* **2011,** *42*, 1727.

16. Grishanov, S. A.; Harwood, R. J.; Booth, I. *Ind. Crop. Prod.* **2006,** *23*, 273.
17. Nystrom, B.; Joffe, R.; Langstrom, R. *J. Reinforced Plast. Compos.* **2007,** *26*, 579.
18. Keller, A. *Compos. Sci. Technol.* **2003,** *63*, 1307.
19. Puglia, D.; Terenzi, A.; Barbosa, S. E.; Kenny, J. M. *Compos. Interfaces* **2008,** *15*, 111.
20. Quijano-Solis, C.; Yan, N.; Zhang, S. Y. *Compos. Pt. A-Appl. Sci. Manuf.* **2009,** *40*, 351.
21. Vergnes, B.; Berzin, F. *Plast. Rubber Compos.* **2004,** *33*, 409.
22. Inceoglu, F.; Ville, J.; Ghamri, N.; Pradel, J. L.; Durin, A.; Valette, R.; Vergnes, B. *Polym. Compos.* **2011,** 32, 1842.
23. Vergnes, B.; Della Valle, G.; Delamare, L. *Polym. Eng. Sci.* **1998,** *38*, 1781.
24. Wu, D.; Wu, L.; Sun, Y.; Zhang, M. *J. Polym. Sci. Pt. B-Polym. Phys.* **2007,** *45*, 3137.
25. Miltner, H. E.; Watzeels, N.; Block, C.; Gotzen, N. A.; Van Assche, G.; Borghs, K.; Van Durme, K.; Van Mele, B.; Bogdanov, B.; Rahier, H. *Eur. Polym. J.* **2010,** *46*, 984.
26. Wollerdorfer, M.; Bader, H. *Ind. Crop. Prod.* **1998,** *8*, 105.
27. Le Moigne, N.; van den Oever, M.; Budtova, T. *Compos. Pt. A-Appl. Sci. Manuf.* **2011,** *42*, 1542.
28. Carvalho, M. G.; Ferreira, P. J.; Martins, A. A.; Figueiredo, M. M. *Tappi J.* **1997,** *802*, 137.
29. Zhang, J. J.; Park, C. B.; Rizvi, G. M.; Huang, H. X.; Guo, Q. P. *J. Appl. Polym. Sci.* **2009,** *113*, 2081.
30. Gimenez, J.; Cassagnau, P.; Michel, A. *J. Rheol.* **2000,** *44*, 527.
31. Godard, F.; Vincent, M.; Agassant, J. F.; Vergnes, B. *J. Appl. Polym. Sci.* **2009,** *112*, 2559.
32. Rodrigez, F., Ed. Principles of Polymer Systems; Taylor & Francis: Washington, DC, **1996.**
33. Salmen, L.; Olsson, A. M. *J. Pulp Pap. Sci.* **1998,** *24*, 99.
34. Lenth, C. A.; Kamke, F. A. *Wood Fiber Sci.* **2001,** *33*, 492.
35. Ruifeng, Y. PhD thesis, Université de Nantes **2012.**
36. Bergander, A.; Salmen, L. *J. Mater. Sci.* **2002,** *37*, 151.
37. Smith, I.; Landis, E.; Gong, M., Eds. Fracture and Fatigue in Wood; Wiley: Chichester, **2003.**
38. Sousa, R. A.; Reis, R. L.; Cunha, A. M.; Bevis, M. *J. Plast. Rubber Compos.* **2004,** *33*, 249.
39. Mano, B.; Araujo, J. R.; Spinace, M. A. S.; De Paoli, M. A. *Compos. Sci. Technol.* **2010,** *70*, 29.
40. Iannace, S.; Ali, R.; Nicolais, L. *J. Appl. Polym. Sci.* **2001,** *79*, 1084.
41. Nitz, H.; Semke, H.; Landers, R.; Mülhaupt, R. *J. Appl. Polym. Sci.* **2001,** 81, 1972.
42. Madsen, B.; Thygesen, A.; Lilholt, H. *Compos. Sci. Technol.* **2007,** *67*, 1584.
43. Bos, H. PhD thesis, Technische Universiteit Eindhoven **2004.**
44. Pickering, K. L.; Beckermann, G. W.; Alam, S. N.; Foreman, N. J. *Compos. Pt. A-Appl. Sci. Manuf.* **2007,** *38*, 461.